

## ARTICLE OPEN



# Microbial metabolomic responses to changes in temperature and salinity along the western Antarctic Peninsula

H. M. Dawson<sup>1</sup> , E. Connors<sup>2</sup> , N. G. Erazo<sup>2,3</sup> , J. S. Sacks<sup>1</sup> , V. Mierzejewski<sup>4</sup>, S. M. Rundell<sup>1</sup>, L. T. Carlson<sup>1</sup>, J. W. Deming<sup>1</sup>, A. E. Ingalls<sup>1</sup> , J. S. Bowman<sup>2,3,5</sup> and J. N. Young<sup>1</sup>

© The Author(s) 2023

Seasonal cycles within the marginal ice zones in polar regions include large shifts in temperature and salinity that strongly influence microbial abundance and physiology. However, the combined effects of concurrent temperature and salinity change on microbial community structure and biochemical composition during transitions between seawater and sea ice are not well understood. Coastal marine communities along the western Antarctic Peninsula were sampled and surface seawater was incubated at combinations of temperature and salinity mimicking the formation (cold, salty) and melting (warm, fresh) of sea ice to evaluate how these factors may shape community composition and particulate metabolite pools during seasonal transitions. Bacterial and algal community structures were tightly coupled to each other and distinct across sea-ice, seawater, and sea-ice-meltwater field samples, with unique metabolite profiles in each habitat. During short-term (approximately 10-day) incubations of seawater microbial communities under different temperature and salinity conditions, community compositions changed minimally while metabolite pools shifted greatly, strongly accumulating compatible solutes like proline and glycine betaine under cold and salty conditions. Lower salinities reduced total metabolite concentrations in particulate matter, which may indicate a release of metabolites into the labile dissolved organic matter pool. Low salinity also increased acylcarnitine concentrations in particulate matter, suggesting a potential for fatty acid degradation and reduced nutritional value at the base of the food web during freshening. Our findings have consequences for food web dynamics, microbial interactions, and carbon cycling as polar regions undergo rapid climate change.

*The ISME Journal* (2023) 17:2035–2046; <https://doi.org/10.1038/s41396-023-01475-0>

## INTRODUCTION

Surface ocean temperatures along the western Antarctic Peninsula (WAP) have increased by  $>1^{\circ}\text{C}$  since the 1950s [1]. Associated changes in sea-ice thickness, extent, and duration have also been observed, along with increased occurrence of freshwater melt ponds and under-ice melt lenses [2, 3]. Glacial ice-mass loss has also contributed to greater freshwater inputs into coastal regions [4], with an observed overall warming and freshening of Southern Ocean waters [5]. The largest glacial ice-mass loss in Antarctica was observed along the WAP [6], where a reduction in sea-ice extent and shorter sea-ice season have also been observed [7–10].

With global air temperatures expected to rise at least  $1\text{--}3^{\circ}\text{C}$  over the next century [11], coastal Antarctic ecosystems will likely be exposed to further warming, freshening, and alterations to seasonal ice dynamics. These changes can be expected to alter the temporal and spatial extent of unique microbial habitats that are created and lost seasonally with the formation and melting of sea ice, from and into the surrounding seawater. Microbial community composition is distinct across these polar environments [12–14], but the mechanistic drivers are not fully understood. In terms of biomass, ice-associated communities are usually dominated by sea-ice algae, which can account for 55–65% of coastal Antarctic primary production [15] and provide fixed carbon to microbes and

higher trophic levels, particularly during winter when primary production in the water column is nearly zero [16]. Newly formed sea-ice algal communities generally resemble the mixed community in the source seawater, while older ice loses centric diatoms and becomes dominated by large pennate diatoms; spring ice shows increasingly mixed communities before diatoms are lost during ice melt, leaving many flagellates [14]. Prokaryotic taxa are similarly distinct, with newly formed sea-ice communities often dominated by Alphaproteobacteria and Archaea, resembling source seawater, and spring ice shifting to dominance by Gammaproteobacteria and Flavobacteriia [13, 17, 18].

Transitions between polar marine habitats are associated with shifts in light, nutrients, temperature, and salinity [19–22]. However, the combined role of temperature and salinity in shaping community composition among polar microorganisms, and the organic matter they use and produce, has not been fully explored. Limited work in sea ice has shown that moderate differences in temperature ( $-1.8$  to  $-0.5^{\circ}\text{C}$ ), with associated changes in salinity, correlate with differences in community composition for protists and bacteria [17]. Culture studies of polar microalgae have shown physiological adaptations to shifting environments, including changes in ribosome and protein abundance, enzyme activity, fatty acid content and composition,

<sup>1</sup>School of Oceanography, University of Washington, Seattle, WA 98195, USA. <sup>2</sup>Scripps Institution of Oceanography, UC San Diego, La Jolla, CA 92037, USA. <sup>3</sup>Center for Marine Biodiversity and Conservation, UC San Diego, La Jolla, CA 92037, USA. <sup>4</sup>School of Earth and Space Exploration, Arizona State University, Tempe, AZ 85287, USA. <sup>5</sup>Center for Microbiome Innovation, UC San Diego, La Jolla, CA 92037, USA. email: hmdawson@uw.edu; youngjn@uw.edu

Received: 18 November 2022 Revised: 28 June 2023 Accepted: 30 June 2023

Published online: 15 September 2023

**Table 1.** Summary of samples collected and analyzed in this study.

Date	Sample type	Sample name	Latitude	Longitude	n	T (°C)	S (ppt)	PAR ( $\mu\text{mol m}^{-2} \text{s}^{-1}$ )
2018-11-05	Sea-ice meltwater	Meltwater	-64.78	-64.05	3	-0.7	25.0	320
2018-11-08	Seawater	SW_08	-64.78	-64.07	3	-0.9	35.7	305
2018-11-12	Seawater	SW_12	-64.78	-64.07	3	-0.7	35.2	375
2018-11-15	Seawater	SW_15	-64.78	-64.07	3	-0.3	35.2	1100
2018-11-17	Seawater	SW_17	-64.78	-64.07	3	-0.1	35.2	850
2018-11-19	Seawater	SW_19	-64.78	-64.07	3	0	35.2	700
2018-11-19	Sea ice	Sea ice_1	n.d.	n.d.	3	n.d.	12.0 <sup>a</sup>	n.d.
2018-11-14	Sea ice	Sea ice_2	n.d.	n.d.	1	n.d.	15.0 <sup>a</sup>	n.d.
2018-11-20	Sea ice	Sea ice_3	n.d.	n.d.	1	n.d.	20.0 <sup>a</sup>	n.d.
2018-11-20	Incubation treatment Meltwater	Meltwater_T-S	n.a.	n.a.	3	3	21.0	100
2018-11-20	Incubation treatment Seawater	SW_T-S	n.a.	n.a.	3	0	35.0	100
2018-11-21	Incubation treatment Sea ice	Sea ice_T-S	n.a.	n.a.	3	-3	52.0	100

n.d., not determined, n.a., not applicable.

<sup>a</sup>Salinity measured following ice-core melt into filtered seawater.

production of ice-binding proteins and exopolymers, and alterations in compatible solute concentrations (for review, see [23, 24]), but observations from mixed natural communities remain limited.

Compatible solutes, or osmolytes, are small organic molecules in a cell's cytosol that maintain turgor pressure and stabilize enzymes; they also play other roles [25, 26]. For example, they act as cryoprotectants in polar microalgae by reducing the intracellular freezing point and maintaining protein hydration spheres [27]. Polar diatoms in culture accumulate compatible solutes to high intracellular concentrations (~1 M) in a taxon-specific manner and alter concentrations as a function of temperature or salinity [28–33]. Direct measurements of compatible solutes in polar environments are rare, but previous work suggests that many are similarly abundant in diatom-dominated sea ice and sea-ice diatom cultures [30].

Compatible solutes contribute to the larger pool of intracellular metabolites. Although marine particulate organic matter is composed largely of macromolecules [34], small polar metabolites, including compatible solutes, are the main component of the aqueous cytosol of cells in particulate organic matter [35]. These metabolites are considered a currency of the microbial loop [36], with roughly half of annual net primary production in the ocean rapidly cycling through as labile dissolved organic carbon compounds (DOC; e.g. metabolites) that are oxidized by heterotrophs [37]. Metabolites serve as carbon, nutrient, and energy sources for heterotrophic bacteria [38, 39], but also mediate phytoplankton-bacteria interactions, serve as predator repellants, manage redox stress, and more [35, 40, 41]. Measurements of the diversity and concentration of small polar metabolites in natural marine communities are limited [42–44], particularly for polar regions [30], and the plasticity of metabolite concentrations is largely unknown [45]. Intracellular metabolite pools can shift substantially in response to microbial interactions [38], making measurements on whole communities valuable alongside single-organism laboratory studies. Thus, in situ measurement of particulate metabolites and their sensitivity to temperature and salinity change will enhance our understanding of microbial physiology during seasonal transitions between polar marine habitats and the resultant impacts on community membership and chemical composition of marine organic matter.

Here, we characterize community structure and particulate metabolite profiles of bacterial and protist communities in sea-ice meltwater, seawater, and sea ice during austral spring along the WAP, recognizing that both the taxonomic composition of microbial communities and the chemical inventory of metabolites impact the flux of carbon and energy through polar food webs. We also examine the flexibility of metabolite pools in the surface seawater community under temperature and salinity conditions that mimic the formation and melt of sea ice. As polar oceans experience rapid warming, increased freshwater inputs, and shifts in seasonal ice formation and melt, this research serves to deepen our understanding of the potential responses of the microbial communities.

## MATERIALS AND METHODS

### Field sample collections

Sea-ice meltwater, seawater, and sea-ice samples were collected near Palmer Station, Anvers Island, Antarctica in November of 2018 (Table 1). Surface (< 1 m) seawater samples were collected into acid-clean carboys at 5 intervals over an 11-day period (November 8–19) in open water off Bonaparte Point (Station B of the LTER sampling grid; [46]). Sea-ice meltwater was collected into acid-clean carboys as surface water adjacent (< 1 m) to a melting pan of landfast sea ice located in Hero Inlet next to Palmer Station and the Marr Glacier. Sea-ice cores were opportunistically collected in this area from the R/V *Lawrence M. Gould* using a Kovacs MARK II ice auger during LMG1810 (Cruise <https://doi.org/10.7284/907972>). For all ice cores, the bottom 5-cm sections were melted in the dark at 4 °C into prefiltered (0.2  $\mu\text{m}$ ) seawater to avoid osmotic shock and cell lysis. Final

salinities of ice samples following this melt procedure are provided in Table 1. Samples were collected in triplicate for all analyses unless noted otherwise (Table 1).

### Temperature and salinity incubations

On the 12th of November 2018 (sample SW\_12), we collected additional seawater for incubation experiments that simulated temperature (T-salinity (S) conditions of sea-ice meltwater (3°C and salinity 21, designated Meltwater\_T-S), ambient seawater (0°C and salinity 35, SW\_T-S), and sea ice (−3°C and salinity 52, Sea ice\_T-S). Triplicate 10-L polycarbonate carboys were used for each treatment. All samples were enriched with f/2 nutrients with silica [47] to prevent potential nutrient limitation in faster-growing treatments of our closed-bottle experiments, where nutrients cannot be replenished by mixing as they are in situ. Maintaining nutrient replete status in all of our samples was necessary to discern the effects of temperature and salinity, rather than nutrient availability, on community and metabolome compositions. Carboys were incubated for approximately 10 days at 100  $\mu\text{mol photons m}^{-2} \text{s}^{-1}$  light on a 20:4 h light:dark cycle. Incubations were subsampled daily for growth and harvested during exponential growth for the measurements detailed below. For details on incubation set up and monitoring, see Supplementary information.

### Sample processing

Field and incubation samples were processed for particulate metabolomics, DNA sequencing, chlorophyll *a* (Chl *a*), particulate organic carbon and nitrogen (POC, PN), DOC, particulate and dissolved extracellular polysaccharides (pEPS, dEPS), and major nutrients ( $\text{NO}_3^-$ ,  $\text{NO}_2^-$ ,  $\text{NH}_4^+$ ,  $\text{SiO}_4^{4-}$ ,  $\text{PO}_4^{3-}$ ). All methods for the collection and processing of these samples are described in Supplementary information. Temperature, salinity, and photosynthetically active radiation (PAR) were measured using a digital thermometer, refractometer, and Walz US-SQS/L spherical quantum sensor with ULM-500 light meter, respectively.

### Metabolite extraction and LC-MS analysis

Metabolites within the particulate pool were extracted from samples filters using a modified Bligh and Dyer extraction, separated via liquid chromatography with a Waters Acquity I-Class UPLC equipped with either a reversed phase or hydrophilic interaction liquid chromatography column, ionized with electrospray ionization with a Thermo Q-Exactive mass spectrometer, and data was acquired in full scan mode as modified from Boysen et al. (2018). Further details on metabolite extraction and LC-MS analysis are provided in Supplementary information.

### Metabolomic data processing

Metabolite peaks obtained from mass spectrometry were integrated using Skyline for small molecules [48]. Full and abbreviated compound names are listed in Table S1, with abbreviated names used in figures throughout. Integrated peak areas were subject to quality control (Table S2) and normalized to the peak area of internal standards (Table S3) using best-matched internal standard normalization [49]. For details, see Supplementary information.

### Metabolite concentration calculations

Absolute concentrations of 134 compounds were calculated or estimated from peak areas using commercially available standards run in the same batch as our samples, similar to previous work [31, 42, 44]. Full quantification methods are provided in Supplementary information and summarized in Table S1.

### DNA extraction, sequencing, and processing

All methods for DNA extraction, high throughput sequencing, and analysis for unique amplicon sequence variants (ASVs) are given in Supplementary information. The Inverse Simpson alpha diversity index was calculated using the phyloseq package in R [50] following Callahan et al. [51].

### Statistical approaches

All methods for evaluating statistical differences in community structure, metabolite composition, metabolite concentrations, and ancillary measurements between samples are described in Supplementary information. For all statistical analyses, a probability level of  $\leq 0.05$  was used to determine

statistical significance with *p* values corrected for false discovery rate (FDR) [52] where appropriate.

## RESULTS

### Physical environment

Temperature and salinity in our meltwater, seawater, and sea-ice field samples were narrower in range than those imposed in the incubation treatments. Field temperatures for meltwater and seawater ranged between −0.9 and 0°C, while salinity was approximately 25 and 35, respectively (Table 1). PAR varied substantially in the field, ranging from 305 to 1100  $\mu\text{mol photons m}^{-2} \text{s}^{-1}$  (compared to 100  $\mu\text{mol photons m}^{-2} \text{s}^{-1}$  in the treatments; Table 1). Though not measured directly in sea-ice samples, in situ temperature and brine salinity are presumed to be close to seawater [53] and PAR is presumed to be lower than surface seawater due to the attenuation of light in ice. The final salinity of sea-ice samples following the melt procedure for sampling was lower than seawater (Salinity 12–20; Table 1).

### Biological measurements

Surface seawater from Nov 12 was used to inoculate the incubations. After an initial lag, photosynthetic growth was detected in all incubation treatments with specific growth rates of approximately 0.3  $\text{d}^{-1}$  for Meltwater\_T-S and SW\_T-S and 0.2  $\text{d}^{-1}$  for Sea ice\_T-S (Fig. 1A, S1a). The seawater community sampled over Nov 8–19 also showed an increase in biomass (Chl *a* and POC) with an estimated specific growth rate of approximately 0.2  $\text{d}^{-1}$  (Fig. 1A, S1b, Table S4). A slight drawdown of nutrients over the sampling period was observed in both the seawater samples and the incubation treatments, though none reached limiting conditions and there was no clear trend based on treatment condition (Table S4). This maintenance of nutrient replete status across samples allowed for comparison of metabolome and community compositions between treatments with different growth rates based on the impact of temperature and salinity change. Meltwater had comparable biomass (POC, Fig. 1B) and nutrient concentrations (Table S4) to seawater. C:N ratios were generally low (5.2–5.6 in seawater and 6.2 in SW\_T-S and Sea ice\_T-S), with slightly higher values in meltwater and Meltwater\_T-S (7.6 and 8, respectively; Fig. 1C).

### Alpha diversity

Eukaryotic diversity in seawater between Nov 8–12 was initially high (Inverse Simpson's index of 14 for the incubation inoculum SW\_12) and decreased throughout the field sampling period and in incubation bottles as the incubation progressed (Fig. 2A), reaching similarly low diversity (approximately 5) within a similar timeframe (7 and 8–9 days, respectively). Sea ice and meltwater eukaryotic diversity fell within the range found in seawater. The prokaryotic community did not show a clear change in diversity over the sampling period in either seawater or the incubation treatments (Fig. 2B), and meltwater diversity was similar to that in seawater. The prokaryotic sea-ice community, however, was considerably more diverse (Inverse Simpson's index of 30) than all other communities sampled ( $p \ll 0.001$ ).

### Community composition

Diatoms (Bacillariophyta) dominated the eukaryotic community numerically in all samples, regardless of habitat or treatment. The initial seawater community was approximately 50% diatoms, increasing to 80% over the sampling period for both seawater and incubation treatments (Fig. S2). The diatom *Rhizosolenia pungens* dominated in all incubations and increased in seawater (from SW\_08 to SW\_17), though the diatom *Corethron inerme* eventually dominated in seawater (SW\_19; Fig. 3A). In contrast, the taxonomic composition of sea ice was mixed, with higher proportions of the diatom *Fragilariopsis sublineata* and the

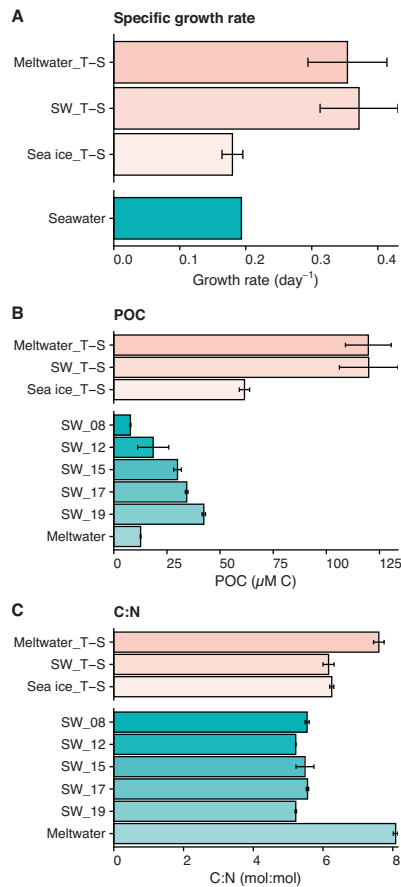


**Fig. 1 General parameters for incubation and field samples.** **A** Specific growth rate (day<sup>-1</sup>) in incubated samples based on exponential change in Chl *a* fluorescence (during days 5–9 for Meltwater\_T-S and Seawater\_T-S, and days 6–10 for Sea ice\_T-S) and in POC (days 6–10) for the seawater field samples; **B** concentration of particulate organic carbon (POC in μM C); and **C** molar ratio of C:N. Error bars represent standard deviation of the mean ( $n = 3$ ). For all plots, y-axis break separates incubation treatment samples on the top (pink) and field samples on the bottom (aqua). Growth curves used to generate specific growth rate are provided in Fig. S1a and b; full data are available in Table S4. Note that we do not have POC or C:N measurements to pair with sea-ice field samples.

dinoflagellate *Pentaparsodinium dalei*, while most meltwater samples were dominated by a raphid pennate diatom. The prokaryotic community was largely bacterial, with the classes Gammaproteobacteria, Alphaproteobacteria, and Flavobacteriia making up the majority of ASVs (Fig. S3). The genus *Polaribacter* was abundant across seawater (increasing in abundance with time), sea-ice, and all incubation samples (Fig. 3B). *Polaribacter* ASVs were less abundant in the meltwater field samples, which were dominated by *Octadecabacter*. Seawater also had high contributions of *Candidatus* Pelagibacter and *Candidatus* Thioglobus (decreasing in abundance with time). Sea-ice bacterial communities were mixed, with large contributions from *Polaribacter*, *Sulfitobacter*, and *Paraglacicola*. Archaeal ASVs were rare, making up 0.05–2% of total reads per sample, and dominated by the phylum Thaumarchaeota. Full ASV abundance data and taxonomic information for 18S and 16S rRNA gene sequencing, including archaeal ASVs, are available in Tables S5 and S6, respectively.

#### Interdependency of prokaryotic and eukaryotic community structures

NMDS ordinations of community structure paired with analysis of similarity (ANOSIM) tests displayed a clear separation of

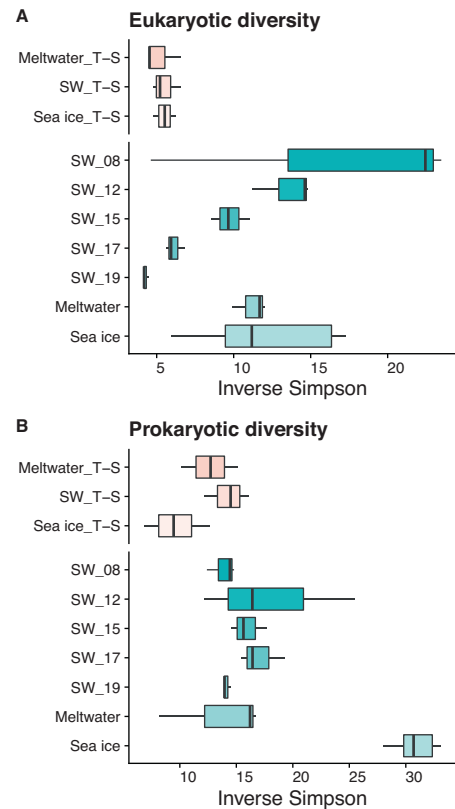


**Fig. 2 Alpha diversity in incubation and field samples.** Inverse Simpson indices of alpha diversity for **(A)** the eukaryotic community and **(B)** the prokaryotic community in both incubation (pink) and field (aqua) samples. In the box plots, the total data range, median, and the 25–75% quartile range (box) are shown. For all plots, y-axis break separates incubation treatment samples on the top and field samples on the bottom.

meltwater, seawater, and sea ice from one another (eukaryotic:  $R = 0.78$ ,  $p < 0.001$ ; prokaryotic:  $R = 0.79$ ,  $p < 0.001$ ), despite one meltwater replicate grouping with seawater (Fig. 4A, B). Seawater samples grouped together in ordination space, though community structure changed significantly over the course of seawater sampling (eukaryotic:  $R = 0.67$ ,  $p < 0.001$ ; prokaryotic:  $R = 0.40$ ,  $p = 0.003$ ). Incubation community structures during harvest were distinct from the initial seawater (eukaryotic:  $R = 0.61$ ,  $p < 0.001$ ; prokaryotic:  $R = 0.88$ ,  $p < 0.001$ ) but did not differ between treatments (eukaryotic:  $R = -0.08$ ,  $p = 0.47$ ; prokaryotic:  $R = 0.12$ ,  $p = 0.23$ ). Full ANOSIM results are listed in Tables S7 and S8.

NMDS ordinations revealed similar patterns within the eukaryotic and prokaryotic community structures (Fig. 4A, B). Symmetric Procrustes analysis revealed a strong, significant congruency among these communities ( $m^2 = 0.14$ ,  $p < 0.001$ ), whereby samples with similar eukaryotic community structures were likely to share similar prokaryotic community structures (Fig. 4C). Correlation analyses based on the Spearman correlation of centered log-ratio-transformed data indicated numerous inter-domain co-occurrences. Across the top 20 eukaryotic and prokaryotic ASVs in our sample set (32 samples), 350 ASV pairings correlated significantly, with 189 correlating positively and 161 negatively (Fig. S4a, Table S9). These pairings included positive correlations between abundant diatom ASVs *Rhizosolenia pungens.12* ( $p = 0.76$ ,  $p = 3.49 \times 10^{-7}$ ) and *Chaetoceros neogracilis.1* ( $p = 0.75$ ,  $p = 9.98 \times 10^{-7}$ ) with *Polaribacter* sp. L3A8.31. Across our field samples (23 samples), significant positive correlations between ASVs aligned largely by habitat type (Fig. S4b): taxa abundant in sea-ice and meltwater samples (e.g. *Sulfitobacter*,



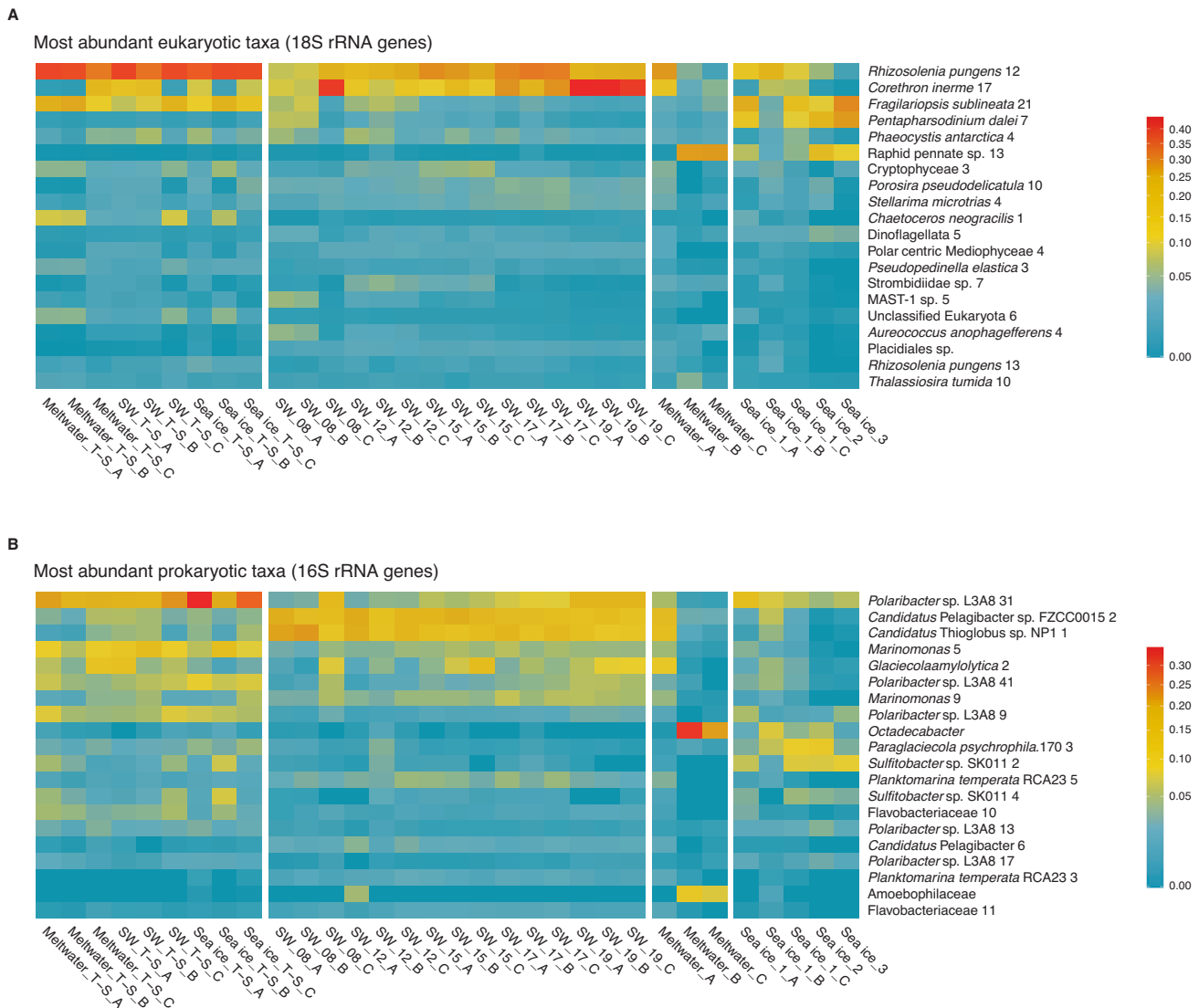


**Fig. 3 Community composition of incubation and field samples.** Color-scaled relative abundance of the 20 most abundant (A) eukaryotic (18S) closest completed genomes (CCGs) and closest estimated genomes (CEGs) and (B) prokaryotic (16S) CCGs and CEGs. Vertical white spaces between samples separate incubation samples for all sample types (left) from field samples by sample type; sample designations \_A, \_B and \_C indicate triplicate samples. Distinct ASVs assigned the same taxonomic name are differentiated by a number following the name (e.g. *Rhizosolenia pungens* 12 versus *Rhizosolenia pungens* 13). Note that the color bars have a square root transformation. Full data available in Tables S5 and S6.

*Octadecabacter*, *Fragilariopsis sublineata*) correlated with each other, while taxa abundant in seawater samples (e.g. *Candidatus Pelagibacter*, *Candidatus Thioglobus*, *R. pungens*) correlated with each other in a separate cluster. Full correlation results can be found in Tables S9 and S10.

### Metabolite pools in polar environments

Particulate pools of 134 known metabolites were quantified (see Table S11). NMDS ordinations paired with ANOSIM tests showed that metabolite profiles clearly separated the meltwater, seawater, and sea-ice samples from each other ( $R = 0.99$ ,  $p \ll 0.001$ ), including a weaker but significant shift over the seawater sampling period ( $R = 0.61$ ,  $p = 1 \times 10^{-4}$ ; Fig. 4D). This distinction by habitat followed the observed pattern in community structure, with samples similar in metabolite composition tending to be similar in eukaryotic and prokaryotic community structure as well (Fig. S5). Unlike community structure, metabolite profiles for incubated samples separated strongly according to treatment ( $R = 0.97$ ,  $p = 0.003$ ), with the control treatment (SW\_T-S)

grouping closely with the in situ seawater samples. When grouped by salinity status, the samples ordered across MDS1, with fresher field samples (meltwater and sea ice) grouping significantly with the Meltwater\_T-S samples as compared to the ambient-salinity seawater or high-salinity Sea ice\_T-S samples (Fig. S6;  $R = 0.89$ ,  $p \ll 0.001$ ). Full ANOSIM results are provided in Table S12.

Total quantified particulate metabolite concentration (as molar carbon concentration, nM C) ranged broadly between field sample types, from approximately 170 nM C in meltwater to 315–1325 nM C in seawater (Fig. S7; Table S14). In our seawater samples, this equates to 2.6–4.0% of POC and 3.1–5.1% of PN, with no clear pattern over the sampling period (Fig. 5B and C, S8 and S9). While SW\_T-S and Sea ice\_T-S metabolite contributions to POC and PN were similar to seawater (approximately 4% POC and 6% PN), both the incubation and field meltwater metabolite pools made up a smaller %POC (approximately 2 and 1.25%, respectively) and %PN (approximately 4 and 2.25%, respectively) (Fig. 5B, C). The 20 most abundant metabolites accounted for about 70% of the total quantified metabolite pool in all samples

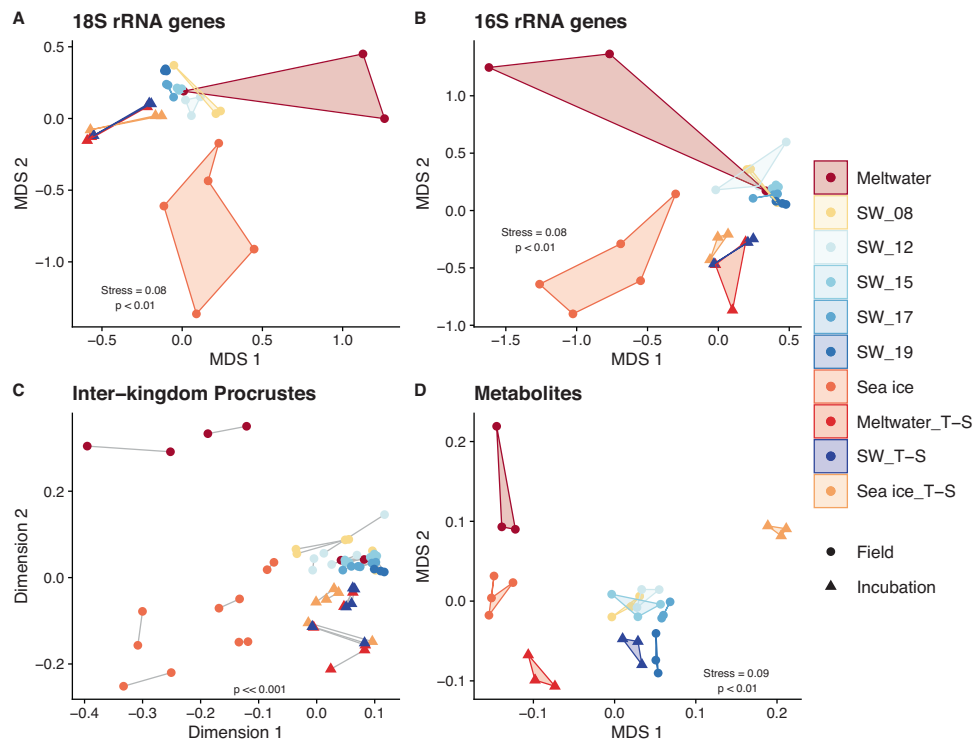


**Fig. 4 Multidimensional structure of community and metabolite composition in incubation and field samples.** Non-metric dimensional scaling (NMDS) ordination, using Bray-Curtis dissimilarities, comparing (A) the eukaryotic (18S) composition and (B) the prokaryotic (16S) composition of each sample. C Procrustes analysis, where points represent individual samples, line connections between points represent eukaryotic and prokaryotic community composition from the same sample, and longer lines indicate greater within-sample dissimilarity between eukaryotic and prokaryotic community structure. D NMDS ordination, using Euclidean distance, comparing the metabolite composition of each sample. Metabolite concentrations (of 134 metabolites) are scaled to mole fraction of carbon. A version of this figure excluding metabolites that were added as part of f/2 nutrients (Cyanocobalamin and Vitamin B1) is available in Fig. S14). Colors indicate sample type. Full data for 18S, 16S, and metabolites are provided in Tables S5, S6, and S11, respectively.

(Fig. 5A), with compatible solutes (e.g. glucosylglycerol, proline, glycine betaine [GBT], dimethylsulfoniopropionate [DMSP].) and free amino acids (e.g. glutamic acid, glutamine, alanine) among the most abundant, similar to previous work [31, 42, 44]. There were clear differences in particulate metabolite composition between the environments sampled and between incubation treatments (Fig. 5A). For example, seawater samples had high contributions (on a mole fraction carbon basis) from glucosylglycerol, proline, glutamic acid, glutamine, and alanine, while sea-ice and meltwater samples had high contributions from arginine and from gonyol and N-acetyl serine, respectively (Figs. 5A and S10). In total, 95 of 134 metabolites contributed significantly to the separation of samples in NMDS ordination space (statistics available in Table S15).

#### Metabolite temperature and salinity sensitivities

Normalizing to POC (nmol metabolite C  $\mu\text{mol C}^{-1}$ ), the concentration of 45 (34%) metabolites differed significantly across temperature and salinity treatments (Fig. 6A; Table S16). Hierarchical clustering (Figs. 6A and S11) indicated that half of those metabolites [23] increased under cold and salty conditions (Sea ice\_T-S) and decreased under warmer and fresher conditions (Meltwater\_T-S) compared to seawater controls (SW\_T-S). Many of these metabolites are known osmolytes (proline, DMSP, GBT). Proline was the most abundant metabolite quantified in our experiment (up to 1.3% of the total POC pool or 29% of the total metabolite C pool in Sea ice\_T-S) and responded strongly to temperature and salinity change: proline was approximately 3 times higher in Sea ice\_T-S ( $p = 0.00042$ ), and 20 times lower in Meltwater\_T-S ( $p = 0.011$ ), compared to SW\_T-S (Fig. 6B). DMSP and GBT were less concentrated than proline (up to 0.3% and 0.1%

of POC, respectively) but responded similarly to temperature and salinity change (Fig. 6C, D).

Many other compatible solutes were present at much lower concentrations (0.00005% to 0.1% of POC) but clustered with proline, DMSP, and GBT, and responded similarly to temperature and salinity change. These include homarine, hypotaurine, taurine, homoserine, dimethylsulfonioacetate (DMS-Ac), ectoine, proline betaine, and betonine (Fig. 6A; Table S11). A few compatible solutes (isethionic acid, gonyol, DHPs) did not show a significant response to temperature and salinity (Fig. S12). Only three metabolites were uniquely enriched under Meltwater\_T-S conditions: cysteic acid, acetyl-L-carnitine, and (iso)butyryl-L-carnitine (Fig. 6A, E, F). Propionyl-L-carnitine followed the same pattern, though the response was not statistically significant (Figs. 6G and S12).

#### DISCUSSION

In this study, the microbial communities of three polar habitats (meltwater, seawater, and sea ice) with distinct physicochemical properties showed unique community structures and taxonomic compositions (Figs. 2–4 and S2–S3). This finding agrees with previous observations [14, 17], with warming spring sea ice associated with mixed pennate diatoms (here, largely *Fragilaria*) and flagellates (here, mainly *Pentaparsodinium*). Centric diatom taxa (*Rhizosolenia* and *Corethron*) became dominant in seawater and all incubation treatments, as commonly observed during phytoplankton blooms in WAP seawater [54–56]. Community structure differed slightly between in situ seawater and our incubations (Fig. 4A, B), which could be driven by the artificial environment of our incubations which included LED lighting and

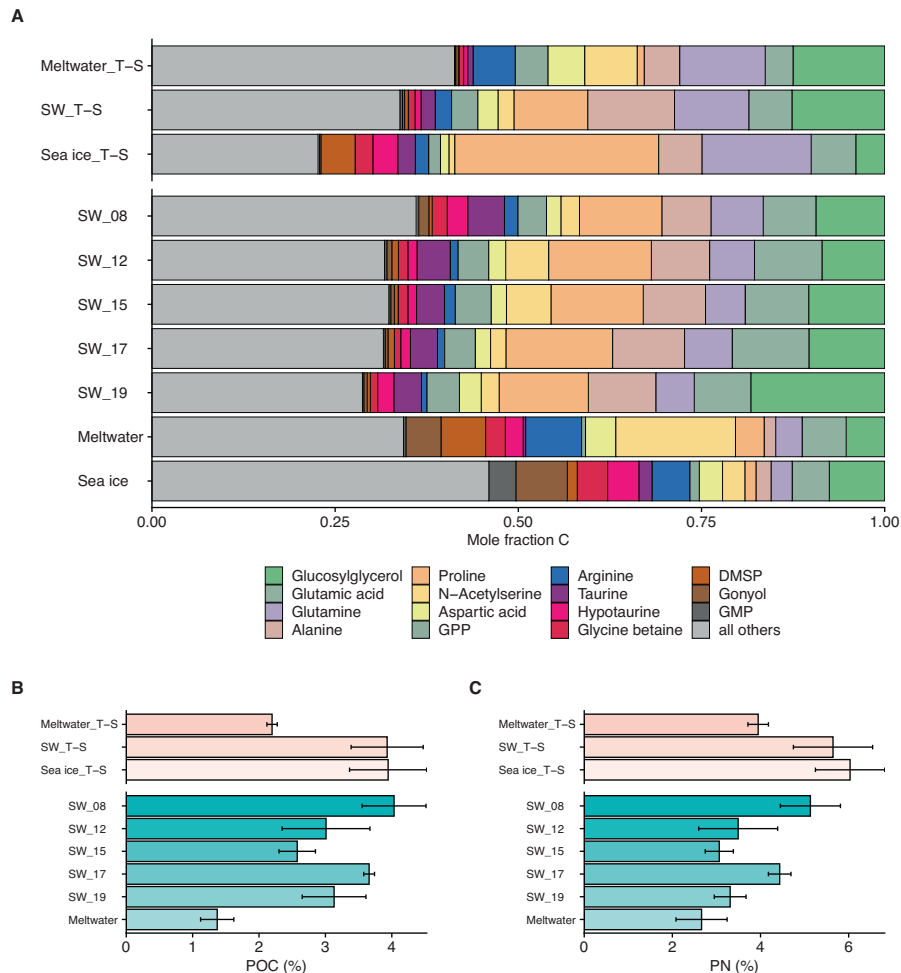


**Fig. 5 Metabolite composition of particulate matter in incubation and field samples.** **A** Metabolite abundance presented as mole fraction of carbon of total identified metabolites [134] across the incubation and field samples. Average of triplicates are shown. The most abundant 15 molecules for each sample are color-coded, with “all others” (gray) containing the sum of the remaining quantified metabolites [119]. Total quantified metabolite concentration as the percentage of **(B)** particulate organic carbon (POC) and **(C)** particulate nitrogen (PN), where error bars represent standard deviation of the mean ( $n = 3$ ). For all plots, y-axis break separates incubation treatment samples on the top and field samples on the bottom. For **(B)** and **(C)**, color denotes incubation (pink) versus field (aqua) samples. Full data available in Table S11; individual metabolite contributions as %POC and %PN, available in Figs. S8 and S9, respectively. Note that we do not have POC or PN to pair with sea-ice field samples.

the addition of f/2 nutrients. However, both had similar dominant algal and bacterial taxa (*Rhizosolenia* and *Polaribacter*, respectively; Fig. 3), suggesting that our incubations remained representative of the seawater community. Numerically, copiotrophic bacteria (*Polaribacter*) overtook oligotrophic taxa (*Candidatus Pelagibacter* [SAR11] and *Candidatus Thioglobus* [SUP05]) during the onset of the phytoplankton bloom in situ (Fig. 3B), as shown previously along the WAP [57] and in the open Southern Ocean [58]. This trend, likely due to faster growth rates of copiotrophs with high availability of labile dissolved organic matter (DOM) [59], was amplified in our closed bottle incubations where DOC was approximately 15 times more concentrated than seawater levels (Table S4 and Fig. S1e).

Microbial community composition is often sensitive to temperature and salinity in sea ice [17] and seawater [60]. Temperature and salinity did not drive community restructuring during our 10-day incubations (Figs. 2–4), possibly due to the length of the experiment or the stability of control variables (light, nutrients, habitable pore space) that often vary alongside temperature and salinity in the environment. Previous studies on polar seawater also suggest that the influence of temperature and salinity on community structure is highly dependent on the

starting community composition [60–62]. Thus, changes in the timing of sea-ice formation and melt could lead to differences in the starting seawater community that will experience temperature and salinity shifts and may alter the resultant microbial community composition.

Congruency between eukaryotic and prokaryotic community structure across all of our samples (Fig. 4C) indicates a consistent coupling between these domains. Algal production and bacterial heterotrophy are tightly coupled in other marine environments [63–65], and specific eukaryotic and prokaryotic taxa have been observed to co-occur in Antarctic sea ice [17, 66] and seawater [67]. Many positive correlations between eukaryotic and prokaryotic ASVs identified here (Fig. S4) are similar to those observed in an Arctic culture study [68] (e.g. a *Chaetoceros* diatom with the flavobacteria *Polaribacter* and a *Fragilariopsis* diatom with the alteromonad *Paraglaciecola*). The specificity of co-occurrences (e.g., *Fragilariopsis sublineata* did not correlate positively with another alteromonad genus, *Glaciecola*) could reflect taxa-specific use of algal exudates by heterotrophic bacteria [68–73]; it could also reflect shared environmental optima rather than direct metabolite exchanges or symbioses. Detecting these inter-domain co-occurrences provides a starting point to target algal-

A

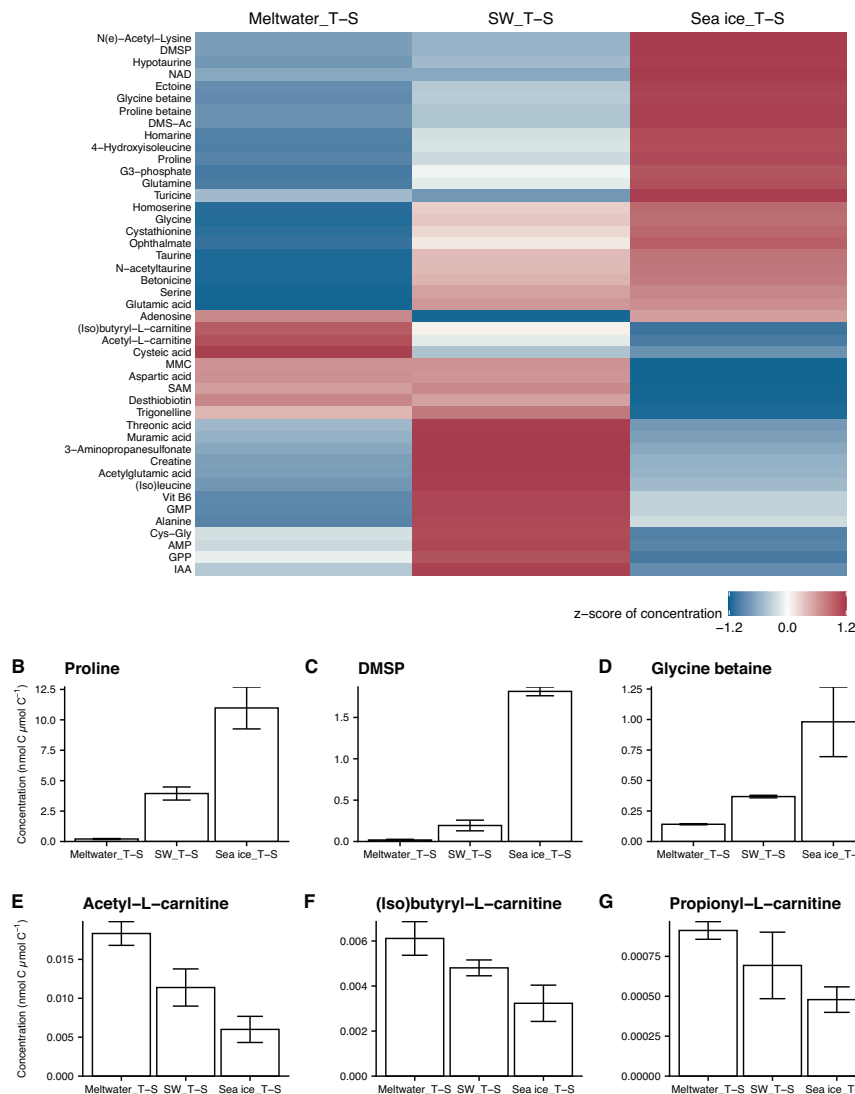


**Fig. 6** Particulate metabolite responses to temperature and salinity change during the incubation experiments. **A** Heat map color-coded by z-score standardized concentrations of 134 metabolites ( $\text{nmol metabolite C } \mu\text{mol C}^{-1}$ ), arranged by average linkage hierarchical clustering of Euclidean distance (dendrogram of clustering available in Fig. S11), for the three different treatments. Compounds listed were each significantly different ( $p < 0.05$ ) with treatment, as determined by false discovery rate-corrected  $p$  values from one-way ANOVAs (detailed in Table S16); compounds not significantly different ( $p > 0.05$ ) are available in Fig. S12. Concentration ( $\text{nmol metabolite C } \mu\text{mol C}^{-1}$ ) of compatible solutes in the incubations, grouped by treatment, for **(B)** proline, **(C)** DMSP, and **(D)** glycine betaine, and of acylcarnitines for **(E)** acetyl-L-carnitine, **(F)** isobutyryl-L-carnitine, and **(G)** propionyl-L-carnitine. Error bars represent standard deviation of the mean ( $n = 3$ ).

bacterial pairs for future studies of microbial interdependencies in polar oceans.

Particulate community metabolomes were distinct across WAP meltwater, seawater, and sea ice (Figs. 4D and 5), following the pattern of community structure (Fig. S5). These metabolome distinctions were likely driven by a combination of habitat-unique taxonomic composition and physicochemical conditions (e.g., salinity, temperature, light). This explanation is consistent with previous seawater and culture studies, where metabolomes reflected community composition or individual taxa identity [31, 44, 74] but were also shaped by physiological responses to environmental conditions [30, 75]. For example, the dinoflagellate compatible solute gonyol [44, 76] was proportionally enriched in our dinoflagellate-rich sea-ice and meltwater samples (Figs. 5 and S10) despite habitat differences in physicochemical factors (Table 1). In contrast, despite only minor changes in microbial

composition throughout our incubation, community metabolomes differed significantly between treatments (Figs. 4D, 5, and 6), suggesting that the seawater taxa present had the metabolic flexibility to adapt to new temperatures and salinities and maintain growth. The experimental control samples maintained at ambient seawater temperature and salinity conditions had markedly similar metabolite profiles and concentrations to the in situ seawater samples (Figs. 4D and 5), which suggests we sampled a nutrient replete system in the early stages of a phytoplankton bloom, where the addition of nutrients alone did not significantly impact metabolome composition within the experiment. Since metabolome composition and concentrations did vary between treatments with the same nutrient availability, we instead conclude that the observed differences were driven largely by temperature and salinity. In this context, our metabolome results suggest that changes in temperature and



salinity could significantly alter polar ocean carbon cycling and microbial interactions mediated by metabolites, even in taxonomically stable and nutrient replete communities. The summed concentrations of metabolites in WAP surface seawater measured here (315–1325 nM C) were higher than those measured in surface marine particles across a North Pacific Ocean transect (68–234 nM C; [44]), but the metabolite contributions to total POC and PN were largely similar, suggesting that the differences could be attributable to the higher biomass in our samples.

Metabolite profiles from the seawater and meltwater incubation treatments were largely similar to their in situ counterparts (Fig. 4D). The Sea ice\_T-S incubation did not group with the sea-ice samples, likely because the incubation conditions resemble wintertime sea ice (higher salinity and lower temperature than seawater), while the brine salinity and temperature of warming spring sea ice we sampled were likely closer to seawater or approaching meltwater upon melt for sampling. This colder and saltier treatment (Sea ice\_T-S) was strongly distinguished by an increased contribution of proline (Fig. S10), a known compatible solute in polar microbe cultures [21, 28–30]. Proline was the most abundant metabolite quantified in our sample set, with seawater concentrations ( $0.5\text{--}1.1\text{ nmol C } \mu\text{mol C}^{-1}$ ) similar to those measured in Arctic sea ice ( $0.5\text{--}1.5\text{ nmol C } \mu\text{mol C}^{-1}$ ; [30]). Proline concentration in POC was elevated 3-fold in the Sea ice\_T-S (Fig. 6), a similar magnitude as in culture studies of two polar diatoms: *Fragilariopsis cylindrus* [28] and *Nitzschia lecontei* [30]. Determining the exact source of this proline (or any metabolite) within POC, which includes total community biomass and detritus, is not possible given the methods of this study, but an increase in metabolite concentration in particulate matter reflects that sources of the metabolite (e.g. biosynthesis, uptake from DOM) are greater than sinks (e.g. catabolism, release as DOM).

Many other metabolites also increased in concentration under cold and salty conditions and decreased in warmer and fresher conditions (Fig. 6), supporting their potential roles in cryo- and osmoprotection [25, 77]. Some of these compounds are likely eukaryotic osmolytes (DMSP; [78–80]), but others are often associated with bacterial taxa (ectoine; [81–83]), reflecting a widespread community response to temperature and salinity change. Along with proline, three of these compounds are abundant in polar diatom cultures and show a similar response to cold and saline conditions: DMSP [30, 32], GBT [30, 33], and homarine [29, 31]. However, the majority have never been quantified or confirmed to be temperature- and salinity-sensitive in culture or in mixed polar marine microbial communities. Thus, the present study has uncovered numerous compounds that deserve more focus as potential compatible solutes (e.g. homoserine, ectoine, DMS-Ac, N(e)-acetyl-lysine; Fig. 6A) in polar contexts, where existing seasonal and future climate-altered shifts in temperature and salinity may impact the standing stocks and cycling of these labile compounds.

Seawater freshening left detectable imprints on organic matter across our samples, with the metabolomes of melt-influenced communities (Meltwater\_T-S, meltwater, sea ice) more similar to each other than to higher salinity samples (seawater, SW\_T-S, Sea ice\_T-S; Fig. S6). Three acylcarnitines—acetyl-L-carnitine, (iso) butyryl-L-carnitine, and propionylcarnitine—accumulated under warm and fresh conditions in our incubation (Fig. 6E–G) and contributed to the separation of field meltwater samples in multivariate space (Fig. S10). Acylcarnitines participate in the transport of fatty acids across mitochondrial membranes for  $\beta$ -oxidation [84], and their accumulation may indicate changes in storage lipid pools, such as the degradation of fatty acids [85]. This possibility aligns with our observation of decreased free concentrations of three essential polyunsaturated fatty acids (PUFAs; arachidonic acid, eicosapentaenoic acid, and docosahexaenoic acid) in low-salinity samples (Fig. S13) and previous observations of PUFA regulation by low salinity in diatoms [86, 87] and Antarctic

phytoplankton [88]. Seawater freshening could thus have important consequences for Antarctic food webs, as the PUFAs produced widely by autotrophs are essential in animal diets [89]. Fatty acid reorganization is also important for maintenance of membrane fluidity in polar microalgae under varying temperature [90] and potentially salinity [91], so this result may also be indicative of membrane restructuring in response to freshening and warming. Alternatively, acylcarnitines may play a role in diatom osmoadaptation or form as a secondary response to changes in amino acid synthesis [92, 93], but these possibilities have yet to be explored in polar microbes.

Freshening also drove reduced total metabolite concentrations, relative to POC and PN, and elevated C:N ratios (Figs. 1 and 5). This low-salinity signature was observed in both our incubation Meltwater\_T-S (salinity 21) and field meltwater (salinity 25) despite differences in community composition, temperature, and nutrient concentrations (Figs. 3, 4A, and 4B; Table S4). Nitrogen limitation or carbon-rich EPS production does not appear to contribute to the higher C:N ratios at lower salinities (Table S4 and Fig. S1c, respectively). This pattern could be due in part to the release of abundant N-rich compatible solutes under hypoosmotic conditions, as shown for GBT in sea-ice algae cultures [33]. However, we estimate that the difference in metabolite concentrations between our freshened and ambient salinity treatments could only drive an approximate 1% change in C:N (6.16 versus 6.21 C:N; calculation in Table S17), much smaller than the difference measured here (23%; Fig. 1C). Differences in C:N were likely driven instead by shifts in abundant macromolecular pools (lipids, carbohydrates, protein) that make up approximately 80% of POC in surface seawater [34].

Although our data suggest that fluctuations in particulate metabolite concentrations are unlikely to alter bulk stoichiometry, they may rapidly alter the composition of labile DOM during increasingly common freshening events. Many metabolites can be respired by the organisms that produce them [42], but others can enter the surrounding dissolved pool via lysis, passive exudation, or active excretion, which has been observed on subsecond timescales in a polar bacterium during freshening [94]. Released N-rich compatible solutes, for example, can be taken up by other microbes and maintained for osmoregulation [33, 95] or catabolized [26, 39]. Microbial metabolism of compatible solutes can lead to the production of marine aerosols, such as monomethylamine or dimethylamine production from GBT via trimethylamine and trimethylamine-N-oxide [96, 97]. Additionally, sulfur-containing compatible solutes (gonyol, DMS-Ac) can inhibit the production of dimethyl sulfide, the primary natural sulfate aerosol precursor, from DMSP [98], suggesting that their release during freshening could alter dimethyl sulfide emissions in polar regions and thus climate regulation [99]. Specific molecular properties of marine DOM (e.g. molecular weight, nitrogen content) likely influence the composition and activity of the microbial community [65, 100], such that environmentally driven changes in DOM composition may alter organic matter cycling, organism interactions, and climate-active marine aerosol production along the WAP.

## CONCLUSION

In the present study, we show that the different marine habitats of sea ice, meltwater, and seawater harbor unique microbial communities distinct in both taxonomy and metabolite composition. Temperature and salinity change drove strong metabolome changes in these coastal WAP communities even in the absence of strong taxonomic change. Mechanistically, they exhibited a marked metabolic flexibility in response to rapid environmental change, the accumulation of compatible solutes under more wintry conditions, and the reverse depletion of those products with regulation of fatty acids under melt conditions. As model predictions in the WAP suggest earlier ice breakup and longer

open water periods with warmer and fresher conditions, our results highlight that a subsequent restructuring of the microbial chemical inventory is possible, likely affecting the fate of organic matter and thus the balance between remineralization and sequestration of atmospheric CO<sub>2</sub>.

## DATA AVAILABILITY

Supporting datasets are provided in the Supplementary Information (Datasets S1–S19). Sequence data are deposited in the National Centre for Biotechnology Information (NCBI) Sequence Read Archive (SRA). 18S and 16S rRNA gene amplicon data are deposited under the NCBI BioProject PRJNA942251. Metabolite data are deposited on Metabolomics Workbench (<https://www.metabolomicsworkbench.org/data/index.php>) under study ID ST002539. All data processing and analysis code is publicly available at [https://github.com/hmdawson/PalmerStation2018\\_Targeted-master](https://github.com/hmdawson/PalmerStation2018_Targeted-master).

## REFERENCES

- Meredith MP, King JC. Rapid climate change in the ocean west of the Antarctic Peninsula during the second half of the 20th century. *Geophys Res Lett*. 2005;32:1–5.
- Arrigo KR, van Dijken G, Pabi S. Impact of a shrinking Arctic ice cover on marine primary production. *Geophys Res Lett*. 2008;35:1–6.
- Arrigo KR, Perovich DK, Pickart RS, Brown ZW, van Dijken GL, Lowry KE, et al. Phytoplankton blooms beneath the sea ice in the Chukchi sea. *Deep Res Part II Top Stud Oceanogr*. 2014;105:1–16.
- Cape MR, Vernet M, Pettit EC, Wellner J, Truffer M, Aki G, et al. Circumpolar deep water impacts glacial meltwater export and coastal biogeochemical cycling along the west Antarctic Peninsula. *Front Mar Sci*. 2019;6:1–23.
- Swart NC, Gille ST, Fyfe JC, Gillett NP. Recent Southern Ocean warming and freshening driven by greenhouse gas emissions and ozone depletion. *Nat Geosci*. 2018;11:836–41.
- Schmidtko S, Heywood KJ, Thompson AF, Aoki S. Multidecadal warming of Antarctic waters. *Science*. 2014;346:1227–31.
- Stammerjohn S, Massom R, Rind D, Martinson D. Regions of rapid sea ice change: An inter-hemispheric seasonal comparison. *Geophys Res Lett*. 2012;39:1–8.
- Stammerjohn SE, Martinson DG, Smith RC, Iannuzzi RA. Sea ice in the western Antarctic Peninsula region: Spatio-temporal variability from ecological and climate change perspectives. *Deep Res Part II Top Stud Oceanogr*. 2008;55:2041–58.
- Harangozo SA. Atmospheric circulation impacts on winter maximum sea ice extent in the west Antarctic Peninsula region (1979–2001). *Geophys Res Lett*. 2006;33:2001–4.
- Vaughan DG, Marshall GJ, Connolley WM, Parkinson C, Mulvaney R, Hodgson DA, et al. Recent rapid regional climate warming on the Antarctic Peninsula. *Clim Change*. 2003;60:243–74.
- Bronselaer B, Winton M, Griffies SM, Hurlin WJ, Rodgers KB, Sergienko OV, et al. Change in future climate due to Antarctic meltwater. *Nature*. 2018;564:53–8.
- Boetius A, Anesio AM, Deming JW, Mikucki JA, Rapp JZ. Microbial ecology of the cryosphere: sea ice and glacial habitats. *Nat Publ Gr*. 2015;13:677–90.
- Bowman JS, Rasmussen S, Blom N, Deming JW, Rysgaard S, Sicheritz-Ponten T. Microbial community structure of Arctic multiyear sea ice and surface seawater by 454 sequencing of the 16S RNA gene. *ISME J*. 2012;6:11–20.
- van Leeuwe MA, Tedesco L, Arrigo KR, Assmy P, Campbell K, Meiners KM, et al. Microalgal community structure and primary production in Arctic and Antarctic sea ice: A synthesis. *Elem Sci Anth*. 2018;6:1–25.
- McMinn A, Pankowski A, Ashworth C, Bhagooli R, Ralph P, Ryan K. In situ net primary productivity and photosynthesis of Antarctic sea ice algal, phytoplankton and benthic algal communities. *Mar Biol*. 2010;157:1345–56.
- Kohlbach D, Graeve M, Lange BA, David C, Schaafsma FL, van Franeker JA, et al. Dependency of Antarctic zooplankton species on ice algae-produced carbon suggests a sea ice-driven pelagic ecosystem during winter. *Glob Chang Biol*. 2018;24:4667–81.
- Torstensson A, Dinasquet J, Chierici M, Fransson A, Riemann L, Wulff A. Physicochemical control of bacterial and protist community composition and diversity in Antarctic sea ice. *Environ Microbiol*. 2015;17:3869–81.
- Collins ER, Rocap G, Deming JW. Persistence of bacterial and archaeal communities in sea ice through an Arctic winter. *Environ Microbiol*. 2010;12:1828–41.
- Dieckmann GS, Thomas DN. Antarctic sea ice – a habitat for extremophiles. *Science*. 2002;295:641–4.
- Ewert M, Deming J. Sea ice microorganisms: Environmental constraints and extracellular responses. *Biol (Basel)*. 2013;2:603–28.
- Ewert M, Deming JW. Bacterial responses to fluctuations and extremes in temperature and brine salinity at the surface of Arctic winter sea ice. *FEMS Microbiol Ecol*. 2014;89:476–89.
- Cox GFN, Weeks WF. Equations for determining the gas and brine volumes in sea-ice sample. *J Glaciol*. 1983;29:306–16.
- Deming JW, Young JN. The role of exopolysaccharides in microbial adaptation to cold habitats. In: Margesin R, editor. *Psychrophiles: from biodiversity to biotechnology*. 2nd ed. Berlin Heidelberg, Germany: Springer-Verlag; 2017. p. 259–84.
- Young JN, Schmidt K. It's what's inside that matters: Physiological adaptations of high-latitude marine microalgae to environmental change. *N. Phytologist*. 2020;227:1307–18.
- Yancey PH, Clark ME, Hand SC, Bowlus RD, Somero GN. Living with water stress: Evolution of osmolyte systems. *Science*. 1982;217:1214–22.
- Welsh DT. Ecological significance of compatible solute accumulation by microorganisms: from single cells to global climate. *FEMS Microbiol Rev*. 2000;24:263–90.
- Lyon B, Mock T. Polar microalgae: New approaches towards understanding adaptations to an extreme and changing environment. *Biol (Basel)*. 2014;3:56–80.
- Krell A, Funk D, Plettner I, John U, Dieckmann G. Regulation of proline metabolism under salt stress in the psychrophilic diatom *Fragilariopsis cylindrus* (Bacillariophyceae). *J Phycol*. 2007;43:753–62.
- Boroujerdi AFB, Lee PA, DiTullio GR, Janech MG, Vied SB, Bearden DW. Identification of isethionic acid and other small molecule metabolites of *Fragilariopsis cylindrus* with nuclear magnetic resonance. *Anal Bioanal Chem*. 2012;404:777–84.
- Dawson HM, Heal KR, Boysen AK, Carlson LT, Ingalls AE, Young JN, et al. Potential of temperature- and salinity-driven shifts in diatom compatible solute concentrations to impact biogeochemical cycling within sea ice. *Elem Sci Anth*. 2020;8:1–17.
- Dawson HM, Heal KR, Torstensson A, Carlson LT, Ingalls AE, Young JN. Large diversity in nitrogen- and sulfur-containing compatible solute profiles in polar and temperate diatoms. *Integr Comp Biol*. 2020;60:1401–13.
- Lyon BR, Bennett-Mintz JM, Lee PA, Janech MG, DiTullio GR. Role of dimethyl-sulfoniopropionate as an osmoprotectant following gradual salinity shifts in the sea-ice diatom *Fragilariopsis cylindrus*. *Environ Chem*. 2016;13:181–94.
- Torstensson A, Young JN, Carlson LT, Ingalls AE, Deming JW. Use of exogenous glycine betaine and its precursor choline as osmoprotectants in Antarctic sea-ice diatoms. *J Phycol*. 2019;70:1–13.
- Lee C, Wakeham S, Arnosti C. Particulate organic matter in the sea: The composition conundrum. *Ambio*. 2004;33:565–75.
- Yancey PH. Organic osmolytes as compatible, metabolic and counteracting cytoprotectants in high osmolarity and other stresses. *J Exp Biol*. 2005;208:2819–30.
- McParland EL, Alexander H, Johnson WM. The osmolyte ties that bind: genomic insights into synthesis and breakdown of organic osmolytes in marine microbes. *Front Mar Sci*. 2021;8:1–20.
- Moran MA, Kujawinski EB, Schroer WF, Amin SA, Bates NR, Bertrand EM, et al. Microbial metabolites in the marine carbon cycle. *Nat Microbiol*. 2022;7:508–23.
- Johnson WM, Kido Soule MC, Kujawinski EB. Evidence for quorum sensing and differential metabolite production by a marine bacterium in response to DMSP. *ISME J*. 2016;10:2304–16.
- Durham BP, Boysen AK, Carlson LT, Groussman RD, Heal KR, Cain KR, et al. Sulfonate-based networks between eukaryotic phytoplankton and heterotrophic bacteria in the surface ocean. *Nat Microbiol*. 2019;4:1706–15.
- Durham BP, Sharma S, Luo H, Smith CB, Amin SA, Bender SJ, et al. Cryptic carbon and sulfur cycling between surface ocean plankton. *Proc Natl Acad Sci*. 2015;112:453–7.
- Amin SA, Hmelo LR, van Tol HM, Durham BP, Carlson LT, Heal KR, et al. Interaction and signalling between a cosmopolitan phytoplankton and associated bacteria. *Nature*. 2015;522:98–101.
- Boysen AK, Carlson LT, Durham BP, Groussman RD, Aylward FO, Ribalet F, et al. Particulate metabolites and transcripts reflect diel oscillations of microbial activity in the surface ocean. *mSystems*. 2021;6:1–18.
- Johnson WM, Longnecker K, Kido Soule MC, Arnold WA, Bhatia MP, Hallam SJ, et al. Metabolite composition of sinking particles differs from surface suspended particles across a latitudinal transect in the South Atlantic. *Limnol Oceanogr*. 2020;65:111–27.
- Heal KR, Durham BP, Boysen AK, Carlson LT, Qin W, Ribalet F, et al. Marine Community Metabolomes carry fingerprints of phytoplankton community composition. *mSystems*. 2021;6:1–19.
- Moran MA. The global ocean microbiome. *Science*. 2015;350:aac8455.

46. Waters KJ, Smith RC. Palmer LTER: A sampling grid for the Palmer LTER program. *Antarct J U S*. 1992;27:236–9.
47. Guillard RRL. Culture of phytoplankton for feeding marine invertebrates. In: Smith WL, Chanley MH, editors. *Culture of Marine Invertebrate Animals*. Boston, MA: Springer; 1975. p. 29–60.
48. MacLean B, Tomazela DM, Shulman N, Chambers M, Finney GL, Frewen B, et al. Skyline: An open source document editor for creating and analyzing targeted proteomics experiments. *Bioinformatics*. 2010;26:966–8.
49. Boysen AK, Heal KR, Carlson LT, Ingalls AE. Best-matched internal standard normalization in liquid chromatography-mass spectrometry metabolomics applied to environmental samples. *Anal Chem*. 2018;90:1363–69.
50. McMurdie PJ, Holmes S. Phyloseq: An R package for reproducible interactive analysis and graphics of microbiome census data. *PLoS One*. 2013;8:1–11.
51. Callahan BJ, Sankaran K, Fukuyama JA, McMurdie PJ, Holmes SP. Bioconductor workflow for microbiome data analysis: From raw reads to community analyses. *F1000Research*. 2016;5:1–50.
52. Benjamini Y, Hochberg Y. Controlling the false discovery rate: a practical and powerful approach to multiple testing. *J R Stat Soc*. 1995;57:289–300.
53. Junge K, Courville Z, Carpenter S, Light B, Lieblappen R, Orellana MV, et al. Physical and optical characteristics of heavily melted “rotten”; Arctic sea ice. *Cryosph Discuss*. 2018;2009:1–30.
54. Annett AL, Carson DS, Crosta X, Clarke A, Ganeshram RS. Seasonal progression of diatom assemblages in surface waters of Ryder Bay, Antarctica. *Polar Biol*. 2010;33:13–29.
55. Schofield O, Saba G, Coleman K, Carvalho F, Couto N, Ducklow H, et al. Decadal variability in coastal phytoplankton community composition in a changing West Antarctic Peninsula. *Deep Res Part I Oceanogr Res Pap*. 2017;124:42–54.
56. Prezelin BB, Hofmann EE, Mengelt C, Klinck JM. The linkage between Upper Circumpolar Deep Water (UCDW) and phytoplankton assemblages on the west Antarctic Peninsula continental shelf. *J Mar Res*. 2000;58:165–202.
57. Bowman JS, Amaral-Zettler LA, Rich JJ, Luria CM, Ducklow HW. Bacterial community segmentation facilitates the prediction of ecosystem function along the coast of the western Antarctic Peninsula. *ISME J*. 2017;11:1460–71.
58. Liu Y, Blain S, Crispi O, Rembauville M, Obernosterer I. Seasonal dynamics of prokaryotes and their associations with diatoms in the Southern Ocean as revealed by an autonomous sampler. *Environ Microbiol*. 2020;22:3968–84.
59. Buchan A, LeClerc GR, Gulvik CA, González JM. Master recyclers: features and functions of bacteria associated with phytoplankton blooms. *Nat Rev Microbiol*. 2014;12:686–98.
60. Antoni JS, Almandoz GO, Ferrario ME, Hernando MP, Varela DE, Rozema PD, et al. Response of a natural Antarctic phytoplankton assemblage to changes in temperature and salinity. *J Exp Mar Bio Ecol*. 2020;532:151444.
61. Hernando M, Varela DE, Malanga G, Almandoz GO, Schloss IR. Effects of climate-induced changes in temperature and salinity on phytoplankton physiology and stress responses in coastal Antarctica. *J Exp Mar Bio Ecol*. 2020;530–531:151400.
62. Piquet AMT, Bolhuis H, Meredith MP, Buma AGJ. Shifts in coastal Antarctic marine microbial communities during and after melt water-related surface stratification. *FEMS Microbiol Ecol*. 2011;76:413–27.
63. Azam F, Malfatti F. Microbial structuring of marine ecosystems. *Nat Rev Microbiol*. 2007;5:782–91.
64. Zhou J, Richlen ML, Sehein TR, Kulis DM, Anderson DM, Cai Z. Microbial community structure and associations during a marine dinoflagellate bloom. *Front Microbiol*. 2018;9:1–21.
65. Kieft B, Li Z, Bryson S, Hettich RL, Pan C, Mayali X, et al. Phytoplankton exudates and lysates support distinct microbial consortia with specialized metabolic and ecophysiological traits. *Proc Natl Acad Sci USA*. 2021;118:1–12.
66. Kaartokallio H, Tuomainen J, Kuosa H, Kuparinen J, Martikainen PJ, Servomaa K. Succession of sea-ice bacterial communities in the Baltic Sea fast ice. *Polar Biol*. 2008;31:783–93.
67. Delmont TO, Hammar KM, Ducklow HW, Yager PL, Post AF. *Phaeocystis antarctica* blooms strongly influence bacterial community structures in the Amundsen Sea polynya. *Front Microbiol*. 2014;5:1–13.
68. Tisserand L, Dadaglio L, Intertaglia L, Catala P, Panagiotopoulos C, Obernosterer I, et al. Use of organic exudates from two polar diatoms by bacterial isolates from the Arctic Ocean: Diatom exudates and Arctic bacteria. *Philos Trans R Soc A Math Phys Eng Sci*. 2020;378:20190356.
69. Tada Y, Nakaya R, Goto S, Yamashita Y, Suzuki K. Distinct bacterial community and diversity shifts after phytoplankton-derived dissolved organic matter addition in a coastal environment. *J Exp Mar Bio Ecol*. 2017;495:119–28.
70. Bertrand EM, McCrow JP, Moustafa A, Zheng H, McQuaid JB, Delmont TO, et al. Phytoplankton-bacterial interactions mediate micronutrient colimitation at the coastal Antarctic sea ice edge. *Proc Natl Acad Sci USA*. 2015;112:9938–43.
71. Amin SA, Parker MS, Armbrust EV. Interactions between diatoms and bacteria. *Microbiol Mol Biol Rev*. 2012;76:667–84.
72. Ferrer-González FX, Widner B, Holderman NR, Glushka J, Arthur S, Kujawinski EB, et al. Resource partitioning of phytoplankton metabolites that support bacterial heterotrophy. *ISME J*. 2020;15:762–73.
73. Dadaglio L, Dinasquet J, Obernosterer I, Joux F. Differential responses of bacteria to diatom-derived dissolved organic matter in the Arctic Ocean. *Aquat Micro Ecol*. 2019;82:59–72.
74. Durham BP, Boysen AK, Heal KR, Carlson LT, Boccamazzo R, Deodato CR, et al. Chemotaxonomic patterns in intracellular metabolites of marine microbial plankton. *Front Mar Sci*. 2022;9:1–17.
75. Heal KR, Kellogg NA, Carlson LT, Lionheart RM, Ingalls AE. Metabolic consequences of cobalamin scarcity in the diatom *Thalassiosira pseudonana* as revealed through metabolomics. *Protist*. 2019;170:328–48.
76. Gebser B, Pohnert G. Synchronized regulation of different zwitterionic metabolites in the osmoadaptation of phytoplankton. *Mar Drugs*. 2013;11:2168–82.
77. Brown AD. Microbial water stress. *Bacteriol Rev*. 1976;40:803–46.
78. Keller MD. Dimethyl sulfide production and marine phytoplankton: the importance of species composition and cell size. *Biol Oceanogr*. 1988;6:375–82.
79. McParland EL, Wright A, Art K, He M, Levine NM. Evidence for contrasting roles of dimethylsulfoniopropionate production in *Emiliania huxleyi* and *Thalassiosira oceanica*. *N. Phytol*. 2020;226:396–409.
80. Karsten U, Kück K, Vogt C, Kirst GO. Dimethylsulfoniopropionate production in phototrophic organisms and its physiological functions as a cryoprotectant. In: Kiene RP, Visscher PT, Keller MD, Kirst Gunter O, editors. *Biological and environmental chemistry of DMSP and related sulfonium compounds*. Boston, MA: Springer US. p. 143–53.
81. Vargas C, Jebbar M, Carrasco R, Blanco C, Calderón MI, Iglesias-Guerra F, et al. Ectoin as compatible solutes and carbon and energy sources for the halophilic bacterium *Chromohalobacter salexigens*. *J Appl Microbiol*. 2006;100:98–107.
82. Kuhlmann AU, Hoffmann T, Bursy J, Jebbar M, Bremer E. Ectoine and hydroxyectoine as protectants against osmotic and cold stress: Uptake through the SigB-controlled betaine-choline-carnitine transporter-type carrier EctT from *Virgibacillus pantothenticus*. *J Bacteriol*. 2011;193:4699–708.
83. Fenizia S, Thume K, Wirgenings M, Pohnert G. Ectoine from bacterial and algal origin is a compatible solute in microalgae. *Mar Drugs*. 2020;18:1–13.
84. Pan Y, Yang J, Gong Y, Li X, Hu H. 3-Hydroxyisobutyryl-coa hydrolase involved in isoleucine catabolism regulates triacylglycerol accumulation in *Phaeodactylum tricornutum*. *Philos Trans R Soc B Biol Sci*. 2017;372:1–10.
85. Boysen A. Marine microbial metabolomics: a journey through time, space, and metabolism [dissertation]. University of Washington; 2020.
86. Chen GQ, Jiang Y, Chen F. Salt-induced alterations in lipid composition of diatom *Nitzschia laevis* (Bacillariophyceae) under heterotrophic culture condition. *J Phycol*. 2008;44:1309–14.
87. Torstensson A, Jiménez C, Nilsson AK, Wulff A. Elevated temperature and decreased salinity both affect the biochemical composition of the Antarctic sea-ice diatom *Nitzschia lecontei*, but not increased pCO<sub>2</sub>. *Polar Biol*. 2019;42:2149–64.
88. Hernando M, Schloss IR, Almandoz GO, Malanga G, Varela DE, De Troch M. Combined effects of temperature and salinity on fatty acid content and lipid damage in Antarctic phytoplankton. *J Exp Mar Bio Ecol*. 2018;503:120–8.
89. Brett MT, Müller-Navarra DC. The role of highly unsaturated fatty acids in aquatic foodweb processes. *Freshw Biol*. 1997;38:483–99.
90. Teoh ML, Phang SM, Chu WL. Response of Antarctic, temperate, and tropical microalgae to temperature stress. *J Appl Phycol*. 2013;25:285–97.
91. An M, Mou S, Zhang X, Zheng Z, Ye N, Wang D, et al. Expression of fatty acid desaturase genes and fatty acid accumulation in *Chlamydomonas* sp. ICE-L under salt stress. *Bioresour Technol*. 2013;149:77–83.
92. Nikitashina V, Stettin D, Pohnert G. Metabolic adaptation of diatoms to hypersalinity. *Phytochemistry*. 2022;201:113267.
93. Peluso G, Barbarisi A, Savica V, Reda E, Nicolai R, Benatti P, et al. Carnitine: An osmolyte that plays a metabolic role. *J Cell Biochem*. 2000;80:1–10.
94. Firth E, Carpenter SD, Sørensen HL, Collins RE, Deming JW. Bacterial use of choline to tolerate salinity shifts in sea-ice brines. *Elem Sci Anth*. 2016;4:000120.
95. Kiene RP, Hoffmann Williams LP. Glycine betaine uptake, retention, and degradation by microorganisms in seawater. *Limnol Oceanogr*. 1998;43:1592–603.
96. Boysen AK, Durham BP, Kumler W, Key RS, Heal KR, Carlson LT, et al. Glycine betaine uptake and metabolism in marine microbial communities. *Environ Microbiol*. 2022;24:2380–403.
97. Chen Y, Patel NA, Crombie A, Scrivens JH, Murrell JC. Bacterial flavin-containing monooxygenase is trimethylamine monooxygenase. *Proc Natl Acad Sci USA*. 2011;108:17791–96.
98. Gebser B, Thume K, Schiller F, Steinke M, Pohnert G. Phytoplankton-derived zwitterionic gonyol and dimethylsulfoniacetate interfere with microbial dimethylsulfoniopropionate sulfur cycling. *Microbiol Open*. 2020;9:1–14.

99. Malin G, Turner SM, Liss PS. Sulfur: The plankton/climate connection. *J Phycol.* 1992;28:590–7.
100. Moran MA, Kujawinski EB, Stubbins A, Fatland R, Aluwihare LI, Buchan A, et al. Deciphering ocean carbon in a changing world. *Proc Natl Acad Sci USA.* 2016;113:3143–51.

## ACKNOWLEDGEMENTS

We would like to thank Ben Van Mooy for the opportunity to sample sea ice; Rebecca Trinh, Jack Conroy, and Shawnee Traylor-Biglio for help with sample collection during the 2018 field season at Palmer Station; Shelly Carpenter for performing EPS measurements; Aaron Morello and the UW Marine Chemistry Lab for assistance with CHN, nutrient, DOC, and chlorophyll analysis; Katherine Heal and Angie Boysen for data processing advice; Will Kumler for statistics and figure advice; Rachel Liu for figure design advice; and the staff of Palmer Station for their assistance.

## AUTHOR CONTRIBUTIONS

HMD and JNY developed the study design. HMD and SMR conducted environmental sampling. HMD, VM, LTC, and JSS performed the metabolite sample processing and analysis. HMD, EC, NGE, and JSB performed the 18S and 16S rRNA sequence sample processing and analysis. HMD, EC, NGE, JSS, SMR, AEI, JWD, and JNY contributed to data interpretation and visualization. HMD and JNY drafted the paper and incorporated revisions from all authors.

## FUNDING

This work was supported by grants from the National Science Foundation (OPP 1744645 to JNY and JWD; OPP 1846837 to JSB; GRFP to SMR), the Simons Foundation (561654 to JNY; 329108 and 385428 to AEI), and the Alfred P. Sloan Foundation (Research Fellowship to JNY).

## COMPETING INTERESTS

The authors declare no competing interests.

## ADDITIONAL INFORMATION

**Supplementary information** The online version contains supplementary material available at <https://doi.org/10.1038/s41396-023-01475-0>.

**Correspondence** and requests for materials should be addressed to H. M. Dawson or J. N. Young.

**Reprints and permission information** is available at <http://www.nature.com/reprints>

**Publisher's note** Springer Nature remains neutral with regard to jurisdictional claims in published maps and institutional affiliations.



**Open Access** This article is licensed under a Creative Commons Attribution 4.0 International License, which permits use, sharing, adaptation, distribution and reproduction in any medium or format, as long as you give appropriate credit to the original author(s) and the source, provide a link to the Creative Commons license, and indicate if changes were made. The images or other third party material in this article are included in the article's Creative Commons license, unless indicated otherwise in a credit line to the material. If material is not included in the article's Creative Commons license and your intended use is not permitted by statutory regulation or exceeds the permitted use, you will need to obtain permission directly from the copyright holder. To view a copy of this license, visit <http://creativecommons.org/licenses/by/4.0/>.

© The Author(s) 2023